Plot-level reconstruction of 3D tree models for aboveground biomass estimation

Guangpeng Fan[a,b], Zhenyu Xu[a], Jinhu Wang[c], Liangliang Nan[d], Huijie Xiao[e], Zhiming Xin[f], Feixiang Chen[a,*]

[a] School of Information Science and Technology, Beijing Forestry University, Beijing 100083, China
[b] Beijing Key Laboratory of Urban Spatial Information Engineering, Beijing 100038, China
[c] Key Laboratory of Quantitative Remote Sensing Technology, Chinese Academy of Sciences, Beijing 100094, China
[d] 3D Geoinformation Research Group, Faculty of Architecture and the Built Environment, Delft University of Technology, 2628 BL Delft, the Netherlands
[e] School of Soil and Water Conservation, Beijing Forestry University, Beijing 100083, China
[f] Inner Mongolia Dengkou Desert Ecosystem National Observation Research Station/Experimental Center of Desert Forestry, Chinese Academy of Forestry, Dengkou, Inner Mongolia 015200, China

Keywords:
Complex forest structure
Above-ground biomass
Estimation uncertainty
Plot-level
TLS point clouds

A B S T R A C T

Complexity of forest structure is an important factor contributing to uncertainty in aboveground biomass estimates. In this study, we present a new method for reducing uncertainty in forest aboveground biomass (AGB) estimation based on plot-level terrestrial laser scanner (TLS) point clouds reconstruction. The method estimates the total AGB of plots with complex structures after automatically performing the steps of ground point filtering, single tree segmentation, and three-dimensional (3D) structure reconstruction. We used plot data from temperate and tropical forest ecosystems to verify the effectiveness of the method, reconstructing a 1300 m^2 temperate plantation plot and a 5000 m^2 mingled forest plot, respectively. The total biomass of 153 trees in the plantation plot was overestimated by 17.12 %, and the total biomass of 61 trees in the mingled forest plot was underestimated by 10.88 %. We found that the uncertainty of aboveground biomass estimation in tropical forests with more complex structures is not necessarily greater than in plantations. Therefore, in large-scale remote sensing observations of forest biomass, the number or area of plots can be increased to reduce the uncertainty of the results caused by the complex structure. The focus of this study is to explore TLS point clouds modeling methods to reduce the uncertainty in AGB estimation caused by the complexity of forest structures, and to provide reference cases for plot-level point clouds reconstruction methods. Forest ecologists can use this method to regularly observe forest growth and obtain indicators related to forest ecology without destroying trees.

1. Introduction

Mastering the aboveground biomass (AGB) of plots is very important for estimating forest productivity, carbon monitoring and understanding forest growth. The complexity and heterogeneity of forest structure are important factors for the uncertainty of forest AGB estimation. Light detection and ranging (LiDAR) can obtain detailed information about the three-dimensional structure of the forest, providing an effective technical means for the quantitative observation and research of the forest ecosystem (Calders et al., 2020; Guo et al., 2021). The AGB of ground samples can be used as calibration data for forest observations using drones or satellites, so it is necessary to obtain accurate and detailed plot-level biomass (Brede et al., 2019; Hu et al., 2020). Traditional methods for estimating biomass from ground samples rely on allometric equations, and it is difficult to overcome the uncertainty of the results caused by the complexity of the forest structure, which may exceed 30 % in some cases (Aguilar et al., 2019; Chave et al., 2014). Therefore, it is very important to obtain accurate and non-destructive ground reference data. Terrestrial laser scanning (TLS) technology can obtain small-scale detailed forest three-dimensional structure information (Luck et al., 2020; Muumbe et al., 2021). The Quantitative Structural Model (QSM) based on the TLS point clouds provides a nondestructive method for estimating the AGB of a single tree. Combining the volume of a single tree reconstructed by QSM with the

* Corresponding author.
E-mail address: bjfxchen@bjfu.edu.cn (F. Chen).

wood density can further estimate the aboveground biomass of a single tree (de Tanago et al., 2018). However, it is necessary to develop a method to automatically reconstruct the TLS point cloud at the plot level by using QSM and obtain the AGB of the plot.

At present, most public QSM methods only support the reconstruction of a single tree, and the single tree point clouds needs to be manually input into the model when calculating AGB. The QSM presents an opportunity to reduce the uncertainty in results caused by the inability of traditional methods to overcome the complexity of the forest structure. Calders et al. used TreeQSM to estimate the tree volume of 65 eucalyptus trees from the TLS point clouds and combined the wood density to infer AGB. The AGB estimates from the allometric growth equation have low consistency with the reference values, and the total AGB is underestimated by 29.85 %~36.57 % (Calders et al., 2015). Takoudjou et al. used SimpletTree to estimate the AGB of a single tree from TLS point clouds and verified the accuracy of the allometric growth equation using the measurement data of 61 destructive felled trees (Momo Takoudjou et al., 2018).

We have developed a method named AdQSM and reconstructed 29 trees of different species (18 species in total) scanned by TLS in three research locations, and validated the accuracy of AdQSM in tree parameter extraction (Fan et al., 2020). Most tree reconstruction methods are only suitable for scanning point clouds with a single tree, requiring manual or semi-automatic extraction of all trees from the plot-level point clouds. Manually extracting a single tree from a large number of point clouds is very time-consuming and overlapping branches of adjacent trees will make manual separation difficult or unreliable (Luck et al., 2020; de Tanago et al., 2018). Raumonen et al. proposed a method to automatically reconstruct the structure model of each tree in the plot using TLS point clouds and tested it with a British oak plot with a diameter of 30 m and an Australian eucalyptus plot with a diameter of 80 m (Raumonen et al., 2015). However, reconstructing the three-dimensional structure of the plot can provide detailed information on large-scale tree growth, which is very important for forest ecology and management.

This paper proposes a method that can reduce the uncertainty of biomass estimation of ground samples caused by the complex structure. After the method automatically performs the steps of ground point classification, single tree segmentation and structural reconstruction from the TLS point clouds at the plot level, the AGB of the plot can be automatically estimated. The traditional AGB estimation method of plot was limited by the type, size and area of plot. This method overcomes these factors and considers the AGB and spatial distribution of the complex branching structure of the plot. The research purposes and contributions of this paper are as follows: (1) Reconstruction of multiple tree structures from TLS point clouds at plot level; (2) Our method realizes the reconstruction of plot in the research field of tree quantitative structure model; (3) Our method can reconstruct the branches and all individual leaves of a single trees in the plot; (4) Our method can be used as a tool for ecologists to manage and monitor forests.

2. Materials and methods

2.1. Data description

2.1.1. Temperate plantation

The plantation is located in the Haidian District of Beijing, China (40°0′N, 116°20′E). It is a plantation planted with Chinese Sophora japonica, with no or only a small amount of understory grassland and bushes. The density of trees in the plantation is about 1,000 trees per hectare. The study area has an altitude of 48.7 m and a flat topography. It belongs to a temperate humid monsoon climate zone with four distinct seasons, with hot summers and cold winters with little precipitation.

Forest survey data

The traditional forest survey method was used to obtain the DBH and height of all the (*Styphnolobium japonicum*) trees in the circular plot. We used the KTS-44R4LCN total station (Guangzhou Southern Surveying and Mapping Technology Co., ltd.) to measure the tree height based on the principle of triangulation, and the diameter at breast height (DBH) tape measure to measure the DBH of each tree. The DBH ranges from 5.6 cm to 23.6 cm, and the average and standard deviation are 13.4 cm and 4.1 cm, respectively. The tree heights range from 4.91 m to 21.86 m, and the average and standard deviation are 13.44 m and 3.25 m.

Point clouds

We collected plot point clouds of Sophora japonica using FARO FOCUSS150 ground laser scanner (FARO Technologies, Inc.). The horizontal and vertical fields of view of the scanner are 360° and 300° respectively, and the minimum horizontal and vertical steps are 0.009°. Five scanning positions are established within a radius of 20 m from the center of the circular plot, one scanning position is in the center, and the other four scanning positions are around. Distribute 12 highly reflective spheres of artificial targets in the whole plot and ensure that at least three spheres are visible at every-two continuous scanning positions (Fan et al., 2020).

2.1.2. Tropical rainforest

We used a dataset of large trees from the tropical rain forest of Cameroon, Africa, which included TLS point clouds and measurements after tree felling. This data set was contributed by Takoudjou et al. (2018), University of Yaounde, Cameroon, and the data is stored in a folder named “Tree”. The trees came from the Ndélélé district in eastern Cameroon, Africa (4°02′20.77″N, 14°55′49.15″E). The average annual precipitation in this area is between 1500 and 2000 mm, the dry season is obvious, the annual average temperature is 24 °C, and the altitude range is between 600 and 700 m. The data set provides TLS point clouds and corresponding felled measurement data of 61 trees, which were scanned, felled, and weighed.

TLS point clouds

We use the TLS point clouds of 61 trees provided in the dataset, and the point cloud of each tree exists independently. Leica ScanStation C10 (Leica Geosystems Co., ltd., Switzerland) is used to scan the point clouds of trees. It is a time-of-flight scanner system with an operating wavelength of 532 nm. The scanner has a wide field of view, the horizontal and vertical fields of view are 360° and 270°, respectively. The scanning speed is 50,000 points/second, and the scanning resolution is set to 0.05 m at 100 m.

Destructive sampling data

The trees were felled between July 2015 and August 2016, and all sample trees were felled after being scanned. The felled trees cover a wide range of tree sizes and average wood density. These trees belong to 15 different species, with an average height of 33.72 m (±12.41) and an average DBH of 58.37 cm (±41.30). The data set also includes DBH and height measured after felling trees. Table 1 shows the detailed information of 61 trees.

2.2. Preprocessing

Plantation plot

The first step of our method is to filter the input point clouds. Reducing the size of point clouds can reduce the requirements of memory and computing time. In this work, there are two steps to preprocess the point clouds of the plot. The improved asymptotically encrypted triangulation filtering algorithm is used to classify the ground

Table 1
Statistics of large tropical trees from mingled forest plot.

Species	Number	DBH/cm		Tree height/m	
		Min	Max	Min	Max
Annickia chlorantha (Oliv.) Setten & Maas	3	10.8	35.6	12.6	35.5
Baphia leptobotrys Harms	3	33.3	84.7	16.5	31.1
Cylicodiscus gabunensis Harms	5	13.3	173.8	17.6	53.6
Duboscia macrocarpa Bocq.	2	26.3	35	17	39.9
Entandrophragma cylindricum (Sprague)	2	17.2	89.8	16.9	44.7
Eribroma oblongum (Mast.) Pierre ex A. Chev.	4	17.4	105.6	22.2	46.5
Erythrophleum suaveolens (Guill. & Perr.)	5	21.9	119.6	26.4	46.9
Macaranga barteri Müll.Arg.	2	25.3	33.7	26.6	28.4
Mansonia altissima (A. Chev.) A. Chev.	3	24.9	60.6	22.3	42.5
Pentachletra macrophylla Benth.	1	34.1	34.1	23.5	23.5
Petersianthus macrocarpus (P.Beauv.) Liben	6	13.4	64.6	11.1	42.7
Pterocarpus soyauxii Taub.	6	11.1	83.2	12.4	49.4
Pycnanthus angolensis (Welw.) Warb.	4	11.2	55.5	8.7	33.5
Terminalia superba Engl. & Diels	9	12.5	112.6	16.2	51.4
Triplochiton scleroxylon K.Schum.	6	25.4	186.6	27.4	52.8

points, and the digital terrain model is established through the irregular triangulation interpolation algorithm to complete the normalization of the plot point clouds.

Mingled forest plot

Since the 61 trees in the dataset are already individualized, to obtain a mixed forest plot that can be used to test our method, we use the open-source software CloudCompare to manually merge the 61 trees to generate the point clouds of the whole plot. The original ground points have been removed, and finally, a mingled forest plot has been obtained.

2.3. Extract all trees in the plot

The accuracy of tree segmentation will directly affect plot reconstruction. To reconstruct the plots quickly and accurately, we design a voxel-based method to segment the trees in the plots from bottom to top.

2.3.1. Single tree extraction

Clustering and seed points

This paper adopts a bottom-up separation strategy based on seed points (Wang et al., 2018). The tree cluster is divided into individual trees, starting with seed point identification. As the density of trunk point clouds is relatively high, this paper chooses 1.3 m as the initial seed point location. Fig. 1 describes the scene of two tree point cloud clusters. Cluster 1 contains one tree with overlapping point clouds, and cluster 2 contains two trees. Colored cells are the initial seed units of the two clusters. The centroid of all points within the voxel acts as the location of the seed point, transferring the seed label to the topmost neighbor.

Tree individualization

The three-dimensional cuboid clusters are divided into multiple tree clusters or a single tree cluster. Multiple-tree clusters have at least two potential seed points, and the minimum distance between the two seeds is greater than the pre-set value. Seed merging prevents a tree with a larger canopy from being segmented into two or more trees. Identify potential seed cells and merge them. Fig. 2 shows a side view of cluster 2 with two overlapping trees, with resampling resulting in 14 vertical

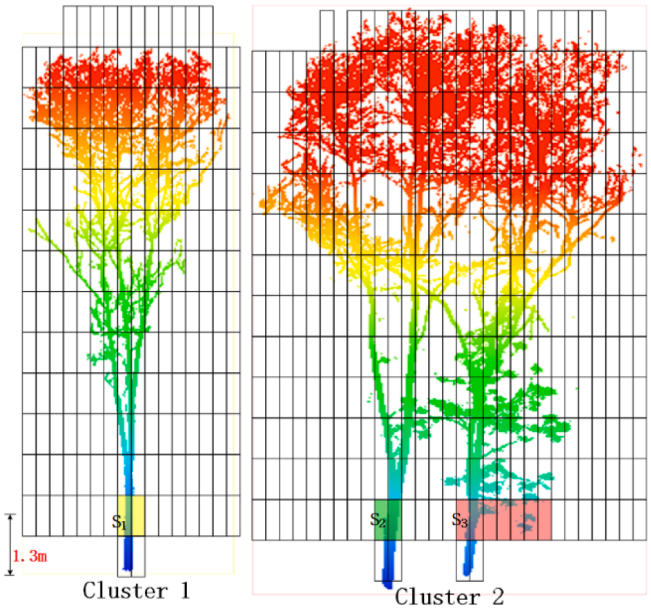

Fig. 1. Cluster potential seed points of individual trees from bottom to top. S_1 is the potential seed of cluster 1; S_2 and S_3 are the potential seeds of cluster 2.

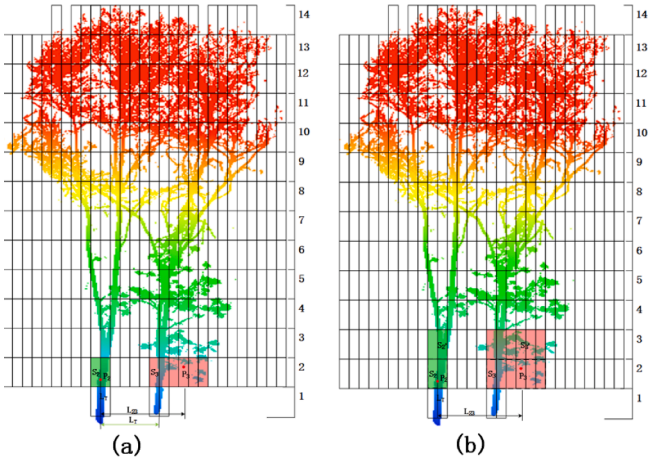

Fig. 2. (a)Recognition and merging of seed points; (b) Inherit the label of the tree from the top layer.

layers. The identified potential seed units were clustered and labeled S_2 and S_3, with P_2 and P_3 being the centroids of seed points in each cluster. The horizontal distance between the two selected seed units is calculated as L_{23}.

In Fig. 2, L_{23} is the distance between two selected seeds, and L_T is the distance threshold of two trees with two trunks. S_2 and S_3 remain unchanged if the horizontal distance L_{23} is greater than L_T. Otherwise, it will be merged into a new seed spot. Then recalculate the distance between seed pairs and repeat the judgment until the distance is not greater than L_T. As shown in Fig. 3, the top neighbors of seeds S_2 and S_3 in layer 2 are identified as green and red units respectively. These units inherit the index of the cluster and form a new seed at the 3 layers. Assign non-seed cells to a single tree. A given cell layer is connected to only one seed cell, and then these cells are assigned to the corresponding tree.

The top units S_1' and S_2' inherit the labels of the bottom adjacent seeds S_1 and S_2.

As shown in layer 13 (Fig. 3), first identify the boundary of two trees in layer 13. Unallocated cells are allocated according to the connection

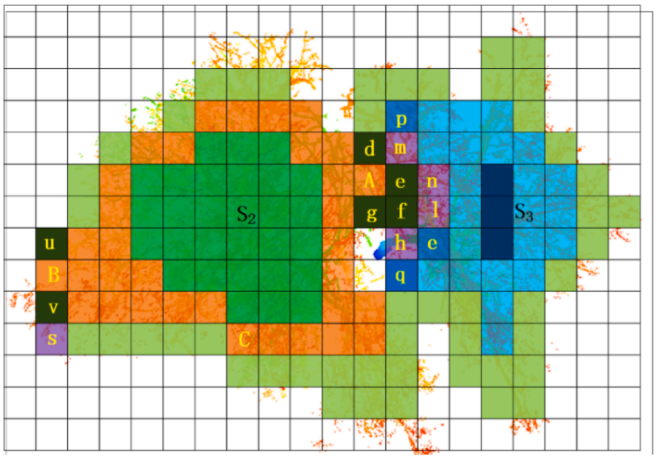

Fig. 3. Cell separation based on neighborhood adjacency.

factor. Set the connection coefficient of all boundary cells to 1 and propagate the connection coefficient to unallocated adjacent cells. As shown in Fig. 3, cells d, e and g are adjacent cells connected by faces, and f is adjacent cells of the edge of boundary cells. Obtain the boundary cells of the seeds S_2 and S_3 to calculate the adjacent coefficients of all unallocated cells (such as d, e, f, and g) in the same layer. The orange and light blue meshes are the boundary cells of seeds S_2 and S_3.

2.3.2. *Tree segmentation results*

Temperate Chinese Sophora japonica Plantation.

As shown in Fig. 4, the point clouds of the Chinese Sophora japonica plot after preprocessing have been segmented. According to the principle of single tree segmentation, the initial value of L_T was set to 50, and 162 individual trees were obtained. The field survey showed that there were 153 trees in the plot. By setting L_T to 65, all trees were successfully obtained in the plot.

Tropical natural rainforest.

As shown in Fig. 5, the trees of the Cameroon rainforest plot had been individualized. The initial value of L_T set was 50, and a total of 56 tree examples have been obtained, and the survey results show that there are a total of 61 trees in the plot. By setting L_T to 90, all trees in the plot are successfully obtained.

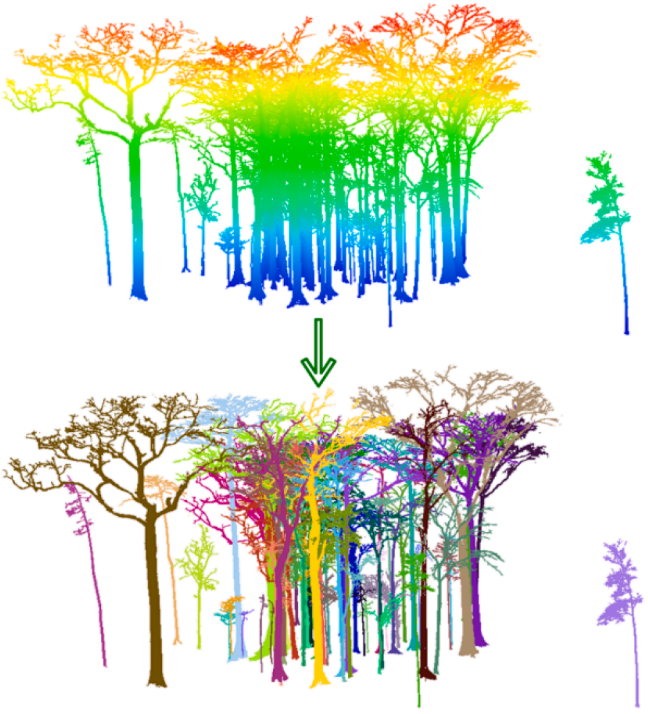

Fig. 5. The method in this paper extracts all the trees in the plantation plot.

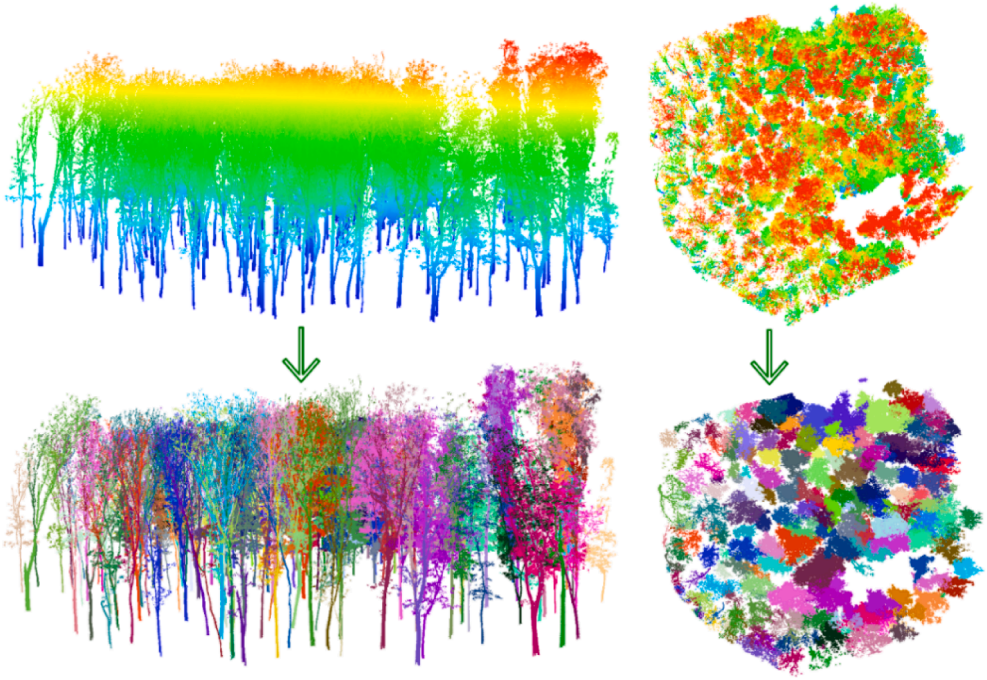

Fig. 4. All trees in the plantation plot were individualized.

2.4. AdQSM reconstructs the 3D structure of tree branches

AdQSM is a method that we have published, it is a new QSM (Dong et al., 2021). AdQSM reconstructs 3D branch geometry structure of a single tree from the TLS point clouds and can quantitatively calculate many attributes of a single tree, such as the volume (diameter, length, number, surface area, etc.) of the branch, clear bole height, diameter at breast height (DBH) and tree height.

AdQSM reconstructs the cylindrical geometric model of a single tree from top to bottom and describes the geometric structure and spatial topological relationship of tree branches from the point clouds based on the tree skeleton (Fig. 6). Combined with ecological theories such as the law of water and nutrient transportation of trees, the tree skeleton is constructed from the internal spatial distribution of the input point clouds (Fig. 6 (a) and (b)), and the Minimum Spanning Tree (MST) algorithm framework is completed to extract trees. The initial skeleton (Fig. 6(c)), a series of skeleton simplification algorithms and optimization strategies such as merging redundant vertices and edges are designed (Fig. 6(d) and (e)). According to the growth law of trees, the cylindrical fitting of the geometric structure of tree branches is completed (Fig. 6(f) and (g)), which is a general and high-precision QSM method.

2.5. Reconstruct multiple trees from the TLS point clouds at the plot level (PlotQSM

First, input the point cloud of each tree into AdQSM in the computer memory. Then, the tree skeleton is initialized, simplified, and smoothed. Finally, install cylinders for the branches of each tree. Reconstruct from bottom to top, first the trunk, then the branches of each grade, and the cylinder of each branch. In the reconstruction process, the trunk point clouds of each tree will be evenly divided into several segments, and the radius of the initial column at the bottom of the trunk will be estimated. Figs. 7 and 8 are the QSM of reconstructed plantation plots and mingled forest plots respectively.

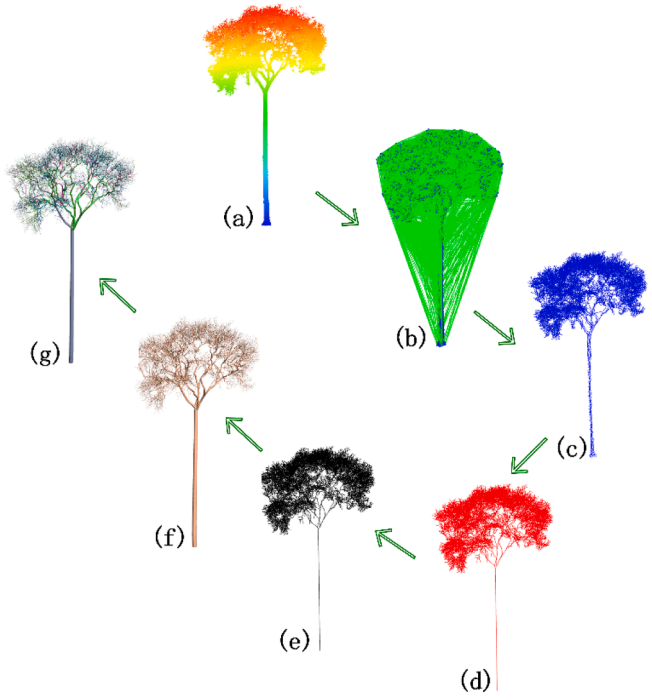

Fig. 6. The main steps of AdQSM to reconstruct a single tree from its TLS point clouds.

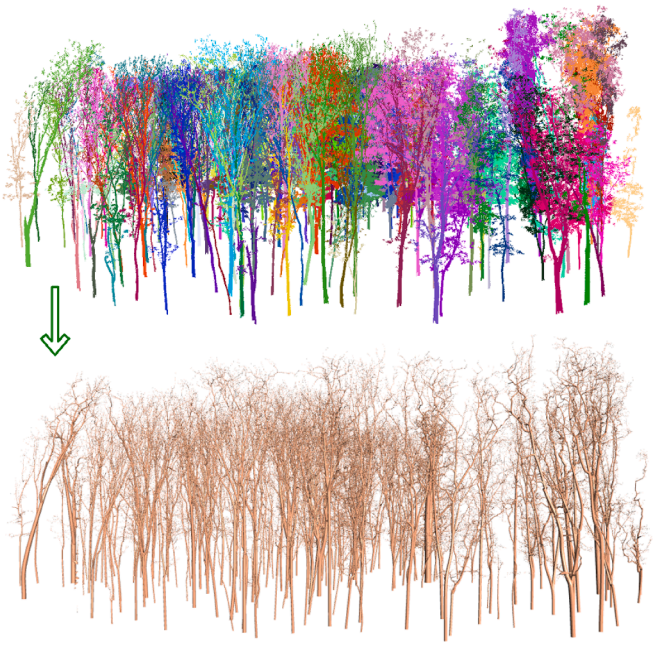

Fig. 7. Quantitative structure model of the plantation plot in the temperate zone.

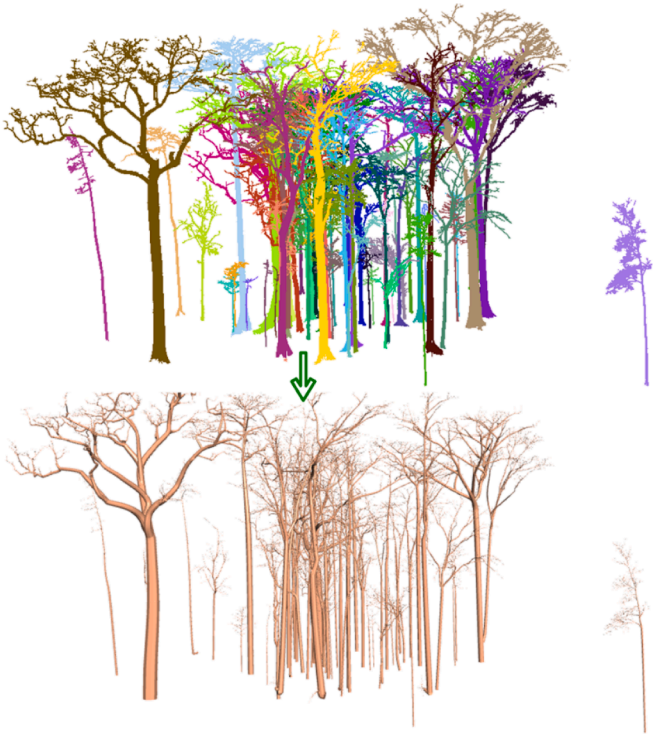

Fig. 8. Quantitative structure model of tropical mingled forest plot.

2.6. Automatic batch extraction of tree volume and AGB from the plot quantitative structure model

For plantation plot and mingled forest plot, the PlotQSM in section 2.5 can automatically extract the volume of all trees. For the two test plots, we generated five plot QSMs, and made five different QSMs for each tree (l = 60, 70, 80, 90, 100 cm). Calculate the dry mass by combining the volume V_{QSM} of the single tree extracted in batches with the wood density WD (Eq. (1)).

$$AGB_{TLS} = V_{QSM} * WD \quad (1)$$

For the plantation plot with 153 trees, to convert the model volume into the dry mass of a single tree, the dried biomass density per fresh volume (0.636 g/cm^3) was extracted from the global wood density database. For the mingled forest plot with 61 trees, the wood density is different due to different tree species (Table 2).

2.7. Validation of our method

AGB of plantation from the allometric equation

This paper uses the results calculated based on the allometric equation as a reference value. In this paper, the allometric equation of robinia pseudoacacia was obtained from national standards and references (Chen et al., 2019), including the biomass of trunks, branches and leaves. The allometric equation describes the estimation of AGB as formula (2).

$$AGB = 0.03D^2H + 0.714 \quad (2)$$

AGB of mingled forest plot after harvest.

The trees in the mingled forest plot are divided into four parts: trunk, branches, buttresses, and leaves (Takoudjou et al., 2018). When the bottom diameter of each section is less than 70 cm, directly weigh it to obtain its fresh weight. For parts with larger diameters, the indirect mass estimation method of volume combined with wood density is used. Use the Smalian formula to estimate the volume of each branch with a length of 1 m. For each wood component (trunk, branch, and stump), a 3 to 5 cm thick round wood sample is collected at the end of one section. Its wood density WD (g/cm^3) and moisture content are estimated in the laboratory after drying in the oven to constant weight. Table 3 shows the total biomass of trees by adding up the dry weights of all segments. For specific information, please refer to the paper that discloses the data.

2.8. Evaluation

The biomass of leaves or fruits is not considered when calculating AGB, which will not affect the accuracy of the test results. According to our statistics, the contribution rate of tropical leaves and fruits to the total biomass does not exceed 1.1 %. When evaluating AGB, we select Bias, rBias, RMSE, and rRMSE as evaluation indicators, and the calculation of each indicator is shown in formulas (3) to (6). The consistency correlation coefficient (CCC) of the variance component estimation based on the R language is used to evaluate the consistency between the AGB extracted from the point clouds of the plot and the reference value.

$$Bias = \frac{1}{n}\sum_{i=1}^{n}(y_i - y_{dest}) \quad (3)$$

$$RMSE = \sqrt{\frac{\sum (y_i - y_{dest})^2}{n}} \quad (4)$$

Table 2
Wood density of each tree in the mingled forest plot.

Category	Common Names	Species	wood density (g/cm^3)
1	*Mubala*	*macrophylla*	0.377534167
2	*Ayous*	*scleroxylon*	0.429883333
3	*Abale*	*macrocarpus*	0.507908824
4	*Ilomba*	*angolensis*	0.337341818
5	*Frake*	*superba*	0.553499333
6	*Ayous*	*scleroxylon*	0.458812308
…	…	…	…
61	*Macaranga*	*barteri*	0.3666

Table 3
AGB of each tree in the mingled forest plot after harvest.

Category	Common Names	Species	Destructive AGB (*Mg*)
1	*Mubala*	*macrophylla*	0.3583105718
2	*Ayous*	*scleroxylon*	18.40735099
3	*Abale*	*macrocarpus*	1.226202463
4	*Ilomba*	*angolensis*	0.026284798
5	*Frake*	*superba*	15.83677709
6	*Ayous*	*scleroxylon*	37.52280806
…	…	…	…
61	*Macaranga*	*barteri*	0.2897169768

$$rBias\% = \frac{Bias}{\bar{y}_r} \times 100\%, \quad (5)$$

$$rRMSE\% = \frac{RMSE}{\bar{y}_r} \times 100\%, \quad (6)$$

where y_i represents the estimated value of the i tree from the plot point clouds; y_{dest} represents the reference value measured after felling the tree; $\bar{y}$ represents the average reference measurement value, and n represents the number of trees.

3. Results

3.1. Plantation plot

For the plantation plot, the total AGB estimated based on the plot reconstruction and the allometric equation were 15889.3 kg and 13566.4 kg. The Bias of AGB was 15.18 kg. Compared with the allometric equation, the total AGB of this plot is overestimated by 17.12 %. Fig. 9 shows the comparison between the AGB of each tree and the reference value from the allometric equation. The R2 of the linear fit between the AGB of each tree and the reference value was 0.79, and there is no significant system deviation from the 1:1 line (the slope is 0.966), The AGB from PlotQSM was evenly distributed on both sides of the reference value. The statistical results show that the RMSE and CV (RMSE) were 36.2 kg and 40.7 % respectively. At the 95 % confidence interval level, the CCC between the AGB and the reference value of the single tree automatically extracted was 0.87, and the LLCI and UICI were 0.83 and 0.90.

Fig. 10 shows the distribution of AGB residues. Most of the residuals of AGB were more evenly distributed on both sides of the y = 0 line, and

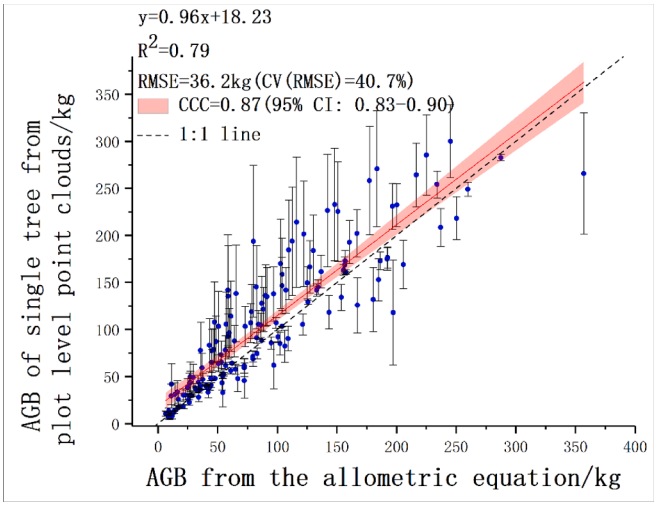

Fig. 9. Comparison of the AGB of each tree extracted from the plot quantitative structure model with the reference value determined from the allometric equation.

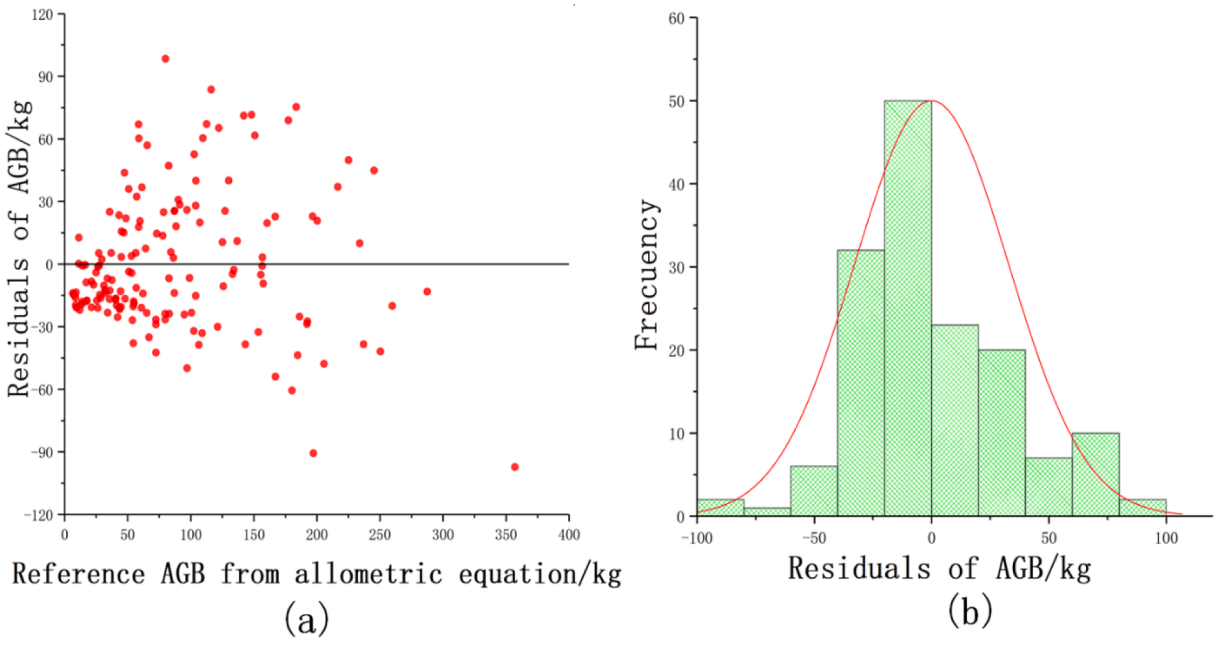

Fig. 10. Distribution of AGB residuals. (a) Scatter; (b) Histogram.

most of the residuals were between −40 kg and 40 kg. The residual value distribution range of AGB has no significant difference with the increase of reference value.

As shown in Table 4, the accuracy of extracting AGB is based on the PlotQSM. The Bias and rBias of AGB calculated by the least square method were 15.18235 kg and 17.12 %. Among the 153 trees with the AGB reference value ranging from 6.4 kg to 357 kg, the trees with an absolute value of deviation less than 36.168 kg accounted for 73.2 % of the total.

In Fig. 11, the absolute deviation of AGB was used as a function of DBH. The absolute deviation of AGB ranges from 0.3 kg to 100 kg. The figure shows that when AGB based on the allometric equation was used as a reference value, the absolute deviation of AGB increases with DBH.

Both DBH and tree height can be used as predictors of AGB, but DBH is still the best predictor of AGB. In some cases, the accuracy of AGB prediction can be improved by considering tree height. Taking the absolute deviation of AGB as a function of DBH and tree height, the absolute deviation of AGB increases with the increase of tree height and DBH (Fig. 12). When the height of the tree was 15 m to 19 m and the DBH was 14 cm to 18 cm, the error of AGB was maximum, but DBH was still the best predictor of AGB. In some cases, the accuracy of AGB prediction can be improve by consideration of tree height.

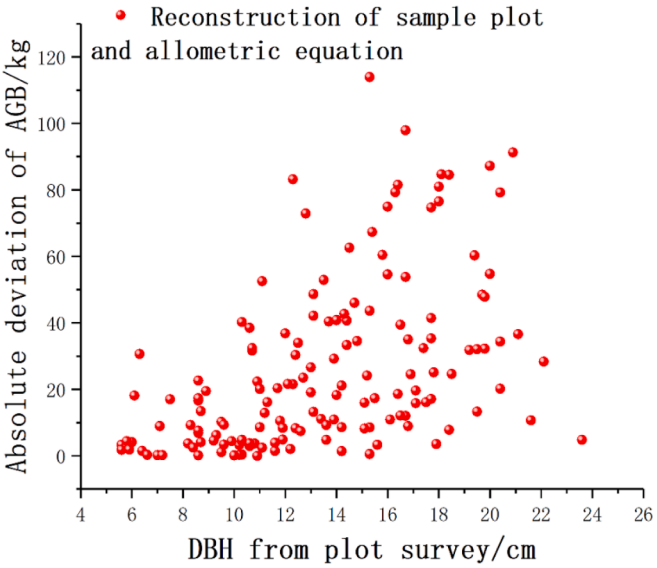

Fig. 11. Absolute deviation of AGB as a function of DBH.

3.2. *Mingled forest plot*

For the mingled forest plot, the total AGB values calculated based on point clouds and destructive sampling were 370.87735 Mg and 416.15445 Mg, respectively. For the reference value, the total AGB was underestimated by 10.88 %. Fig. 13 compares the AGB of each tree with the reference value. The R^2 of the linear fit was 0.98, and the reconstructed AGB was evenly distributed on both sides of the reference value (no major system deviation from the 1:1 line). The slope was 0.93, indicating that the PlotQSM slightly underestimates the AGB of these trees.

The statistical results show that the RMSE was 1.74727 Mg, while the average AGB was 6.82220 Mg, resulting in an rRMSE of 25.61 %. At the 95 % confidence interval level, the AGB extracted by the PlotQSM has a high degree of consistency with the reference value. The CCC was 0.98, the LL CI was 0.97, and the UI CI was 0.99. The error bar was the standard deviation achieved by the QSM model of each tree. The red line represents the linear regression model fitted between the reconstructed AGB and the reference value, and the orange-red band represents the 95 % confidence interval of the regression.

Fig. 14 shows the AGB residual distribution. The residuals of most AGBs were more evenly distributed on both sides of the y = 0 line, and most of the residuals are between −1.5 Mg and 1.5 Mg. Compared with the "big tree" with DBH greater than 60 cm, the reconstruction of the plot level shows less uncertainty and deviation from the reference value for the "small tree" with DBH less than 60 cm. There was no significant

Table 4
Comparison of the AGB of each tree extracted from the PlotQSM and the reference value.

parameter	Bias	rBias (%)	RMSE	rRMSE (%)
AGB (kg)	15.18235	17.12	36.168	40.79

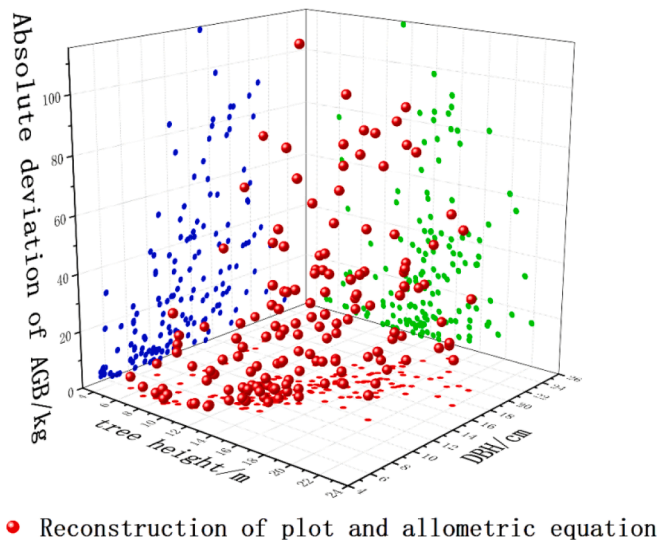

Fig. 12. Absolute deviation of AGB as a function of DBH and tree height.

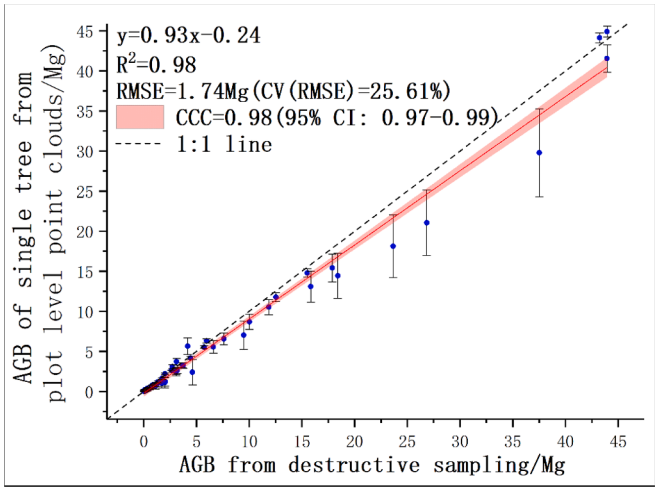

Fig. 13. The AGB of each tree extracted from the PlotQSM compared with the reference value.

difference in the distribution range of the residual value with the increase of the reference value.

As shown in Table 5, the accuracy of AGB is based on the PlotQSM. The Bias and rBias of AGB calculated by the least square method are −0.74225 Mg and −10.88 %. Among the 61 trees whose AGB reference value ranges from 0.02629 Mg to 43.94535 Mg, 85.2 % of the trees whose absolute value of the deviation was less than 1.74727 Mg.

4. Discussion

4.1. PlotQSM can reconstruct TLS point clouds at plot level

The complex structure of forest plots is an important factor leading to the uncertainty of biomass remote sensing observations. This paper proposes a new method (PlotQSM) to reduce the uncertainty of AGB estimation results based on plot-level TLS point cloud. The method estimates the total AGB of plots with complex structures after automatically performing the steps of ground point filtering, single tree segmentation and 3D structure reconstruction. Except for the segmentation errors of individual trees or branches, our method can correctly extract all the trees in the plot. A tropical mingled forest plot and a temperate plantation plot were used to test our method. Based on the volume of trees extracted in batches from the PlotQSM, combined with the wood density, the AGB of the two plots was estimated.

This study can be regarded as a representative of using plot-level TLS point clouds reconstruction to reduce the uncertainty of AGB estimation, and has the potential to reconstruct a larger plot area. Compare our method with existing studies (Raumonen et al., 2015). Firstly, the purpose of reconstructing plot level point clouds is to reduce the uncertainty of AGB estimation. We reconstructed a 1300 m^2 temperate plantation plot and a 5000 m^2 mingled forest plot, and more trees, a larger plot area, and less computation time. The modeling time was about 40 min and 100 min respectively (Windows 10 64-bit, Intel I7-8700 processor, 3.20 GHz and 16 G RAM). Raumonen reconstructed the British oak plot with an area of 700 m^2 and the Australian eucalyptus plot with an area of 5000 m^2 respectively, and the modeling time using laptops (MATLAB, MacBook Pro, 2.8 GHz, 16 GB) was about 100 min and 160 min. Secondly, in the case of more complex structures and larger areas, there is reliable accuracy to reduce the uncertainty of the plot's AGB estimation. The total biomass of 15 trees in the oak plot was overestimated by about 17 % in Raumonen's study, and the total biomass of 27 trees in the eucalypt plot was overestimated by about 8.5 %. The total biomass of 153 trees in the plantation plot was overestimated by 17.12 %, and the total biomass of 61 trees in the mingled forest plot was underestimated by 10.88 %. This method has the potential to be applied to a larger area, even if the requirements for memory and calculation time may increase with the increase of the plot area.

4.2. AdQSM already has the function of realistic 3D reconstruction of leaves and avoids some error sources

Although mixed forest plots have more complex structures, more tree species and larger areas, the accuracy of reconstructing the mingled forest plot is slightly higher than that of the planted forest. Reference values for reconstructed plantation plots are derived from traditional allometric equation estimation methods (Olagoke et al., 2016), while the reference value of the reconstructed mingled forest plot comes from destructive sampling. The reconstruction of mingled forest plots also proves the effectiveness of the method proposed in this paper to reconstruct plot-level point clouds in the estimation of AGB in complex forests.

When extracting forest AGB based on the PlotQSM, it is necessary to obtain the dried mass density per fresh volume from the global wood density database, which may cause some uncertainty when converting the volume of a single tree to AGB. This study did not consider leaf biomass, because previous studies found that it only accounts for a small part of the total AGB (approximately 1 % to 5 %), which will also have a slight impact on the accuracy calculation. We have developed a non-destructive method for calculating leaf biomass, and this method has been integrated into AdQSM, even though this is not the main purpose of this paper. The main processes described in Fig. 15 are as follows: (1) separating the branches and leaves of trees; (2) Single leaf segmentation; (3) Reconstructing the 3D model of all individual leaves and estimating relevant parameters.

The total biomass of the plot based on the non-destructive estimation of the PlotQSM is similar to the expected. Considering uncertain factors such as wood density, tree species, and different forest ecosystems, the difference may be smaller. Overcoming these uncertainty factors in PlotQSM modeling may increase accuracy. The accuracy of our method is affected by not only the accuracy of the automatic reconstruction of the single tree structure but also the automatic tree segmentation method. The accuracy and efficiency of the PlotQSM should be improved as much as possible, such as improving the accuracy of the 3D structure of the tree reconstructed by AdQSM, ensuring the accuracy of single tree segmentation, and optimizing memory usage and time. At the same time, it may not be possible to develop a QSM that can always accurately reconstruct any tree.

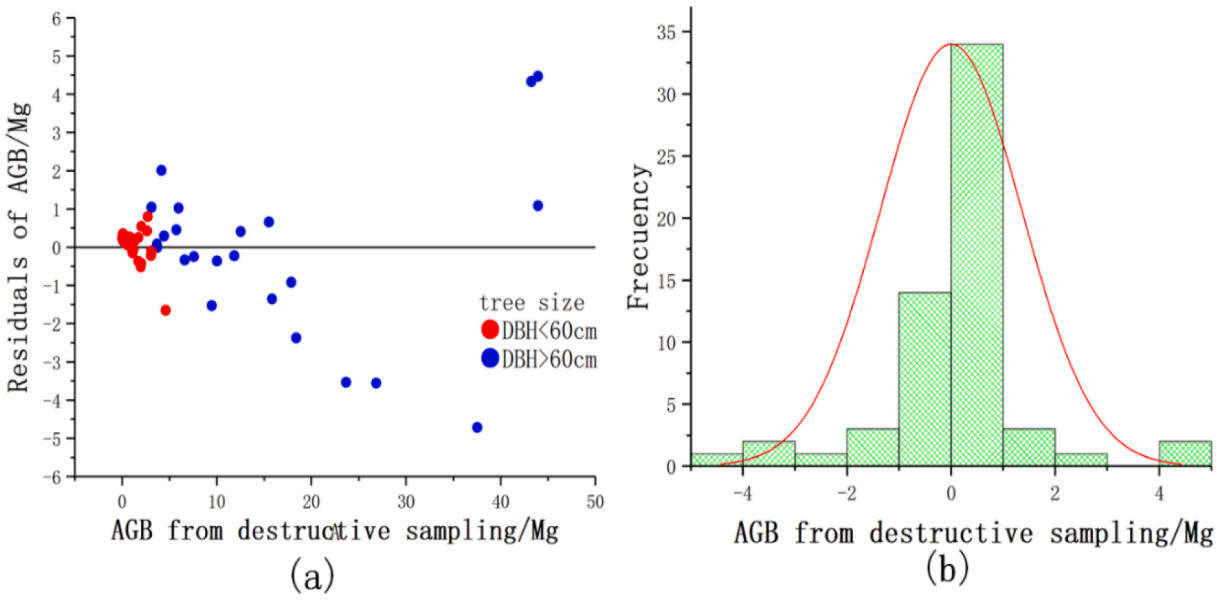

Fig. 14. Distribution of AGB residuals. (a) Scatter distribution of AGB residuals; (b) Histogram of AGB residuals distribution.

Table 5
Accuracy comparison between the AGB of each tree from the PlotQSM and the reference value.

parameter	Bias	rBias (%)	RMSE	rRMSE (%)
AGB (Mg)	−0.74225	−10.88	1.74727	25.61

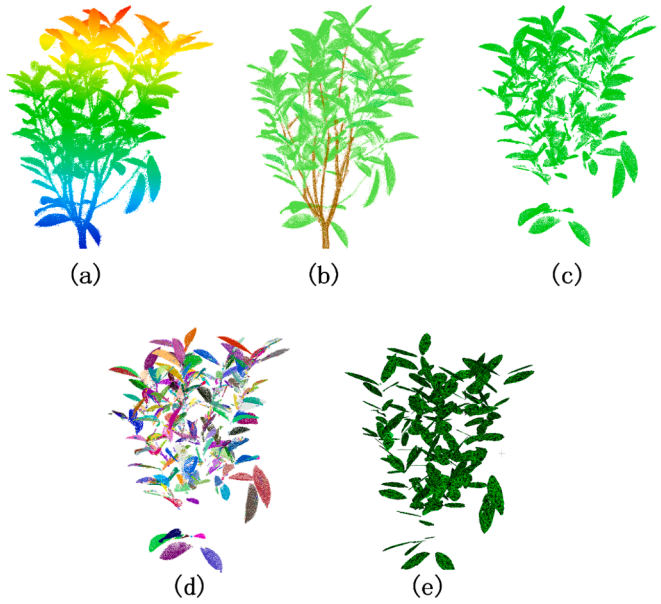

Fig. 15. PlotQSM will further integrate the leaf modeling process. (a)Point clouds of branches and leaves by elevation;(b) Separation of branches and leaves;(c) Leaf point clouds; (d) Single leaf segmentation;(e) All individual leaf reconstruction.

4.3. PlotQSM has multiple functions and application potential

When aerial remote sensing technology such as UAV is used to monitor forest biomass (D'hont et al., 2021; Guo et al., 2017), the " PlotQSM" can be used as a source of reference values (true values) for calibrating aerial measurements. It provides a more flexible approach to ground survey methods in some cases. PlotQSM does not need any information about tree species when calculating forest stocks. With stable accuracy and reliability, it can be used as a ground truth test product for forest ecological remote sensing.

The PlotQSM in this paper can also automatically calculate forest parameters such as crown density, plant number density, average stand height, stand average DBH, cross-sectional area per hectare, and stock volume. At present, mobile laser scanners or UAV laser scanners can quickly and comprehensively scan large areas of forest (Guo et al., 2021; Jurado et al., 2020). Our method is a better starting point for measuring forest structure from these large data sets. Based on the PlotQSM, the real reconstruction of tree leaves can be considered. Combining leaf shape and parameters, the radiation transmission and energy flow of forests can be studied from a three-dimensional perspective, and people's understanding of forest structure, function, and the ecological process can be enriched (Mkaouar et al., 2021, 2021; Song et al., 2021).

5. Conclusions

We propose a reconstruction method based on plot-level TLS point clouds to reduce the uncertainty of AGB estimation due to the complex forest structure. The accuracy, robustness, and efficiency of our method were evaluated using two different types of plots of plantation and mingled forests. We found that the uncertainty of aboveground biomass estimation in tropical forests with more complex structures is not necessarily greater than in plantations, and factors such as the size or area of ground samples may play a major role. In large-scale remote sensing observations of forest biomass, the number or area of plots can be increased to reduce the uncertainty of the results caused by the complex structure. In this paper, the biomass of leaves is not considered in the point cloud reconstruction method at the level of the sample plot. Although PlotQSM has been able to reconstruct all individual leaves of each tree in the sample plot at present, the real reconstruction of the point cloud at the level of the sample plot including leaves and biomass calculation will be considered in the future, and the method in this paper will be open to the public for free. In the future, we will couple leaf traits to adapt to changing conditions, which may contribute to further understanding of the mechanisms underlying the interplay between forest structural diversity, species diversity, and functional diversity.

Funding

This research was jointly funded by the Fundamental Research Funds for the Central Universities (BLX202143), Beijing Key Laboratory of Urban Spatial Information Engineering (NO. 20220109) and the National Natural Science Foundation of China (No. 61771456).

CRediT authorship contribution statement

Guangpeng Fan: Conceptualization, Methodology, Software. **Zhenyu Xu:** Validation, Formal analysis, Investigation. **Jinhu Wang:** Methodology, Software, Writing – review & editing. **Liangliang Nan:** Methodology, Software, Supervision. **Huijie Xiao:** Supervision. **Zhiming Xin:** Supervision. **Feixiang Chen:** Methodology, Software, Supervision, Resources, Funding acquisition.

Declaration of Competing Interest

The authors declare that they have no known competing financial interests or personal relationships that could have appeared to influence the work reported in this paper.

Data availability

Data will be made available on request.

Acknowledgments

We thank the PlotQSM developers and those who worked on the manuscript.

References

Aguilar, F.J., Nemmaoui, A., Pealver, A., Rivas, J.R., Aguilar, M.A., 2019. Developing allometric equations for teak plantations located in the coastal region of ecuador from terrestrial laser scanning data. Forests 10, 1–22. https://doi.org/10.3390/f10121050.

Brede, B., Calders, K., Lau, A., Raumonen, P., Kooistra, L., 2019. Non-destructive tree volume estimation through quantitative structure modelling: Comparing UAV laser scanning with terrestrial LIDAR. Remote Sensing of Environment 233, 111355. https://doi.org/10.1016/j.rse.2019.111355.

Calders, K., Newnham, G., Burt, A., Murphy, S., Raumonen, P., Herold, M., Culvenor, D., Avitabile, V., Disney, M., Armston, J., Kaasalainen, M., McMahon, S., 2015. Nondestructive estimates of above-ground biomass using terrestrial laser scanning. Methods Ecol. Evol. 6 (2), 198–208.

Calders, K., Adams, J., Armston, J., Bartholomeus, H., Bauwens, S., Bentley, L.P., Chave, J., Danson, F.M., Demol, M., Disney, M., Gaulton, R., Krishna Moorthy, S.M., Levick, S.R., Saarinen, N., Schaaf, C., Stovall, A., Terryn, L., Wilkes, P., Verbeeck, H., 2020. Terrestrial laser scanning in forest ecology: Expanding the horizon. Remote Sens. Environ. 251, 112102 https://doi.org/10.1016/j.rse.2020.112102.

Chave, J., Réjou-Méchain, M., Búrquez, A., Chidumayo, E., Colgan, M.S., Delitti, W.B.C., Duque, A., Eid, T., Fearnside, P.M., Goodman, R.C., Henry, M., Martínez-Yrízar, A., Mugasha, W.A., Muller-Landau, H.C., Mencuccini, M., Nelson, B.W., Ngomanda, A., Nogueira, E.M., Ortiz-Malavassi, E., Pélissier, R., Ploton, P., Ryan, C.M., Saldarriaga, J.G., Vieilledent, G., 2014. Improved allometric models to estimate the aboveground biomass of tropical trees. Glob. Change Biol. 20 (10), 3177–3190.

Chen, S., Feng, Z., Chen, P., Ullah Khan, T., Lian, Y., 2019. Nondestructive estimation of the above-ground biomass of multiple tree species in boreal forests of china using terrestrial laser scanning. Forests 10, 936. https://doi.org/10.3390/f10110936.

D'hont, B., Calders, K., Bartholomeus, H., Whiteside, T., Bartolo, R., Levick, S., Krishna Moorthy, S.M., Terryn, L., Verbeeck, H., 2021. Characterising termite mounds in a tropical savanna with UAV laser scanning. Remote Sens. 13 (3), 476.

Dong, Y., Fan, G., Zhou, Z., Liu, J., Wang, Y., Chen, F., 2021. Low cost automatic reconstruction of tree structure by AdQSM with terrestrial close-range photogrammetry. Forests 12, 1020. https://doi.org/10.3390/f12081020.

Fan, G., Nan, L., Dong, Y., Su, X., Chen, F., 2020. AdQSM: a new method for estimating above-ground biomass from TLS Point clouds. Remote Sensing 12, 3089. https://doi.org/10.3390/rs12183089.

Gonzalez de Tanago, J., Lau, A., Bartholomeus, H., Herold, M., Avitabile, V., Raumonen, P., Martius, C., Goodman, R.C., Disney, M., Manuri, S., Burt, A., Calders, K., Kriticos, D., 2018. Estimation of above-ground biomass of large tropical trees with terrestrial LiDAR. Methods Ecol. Evol. 9 (2), 223–234.

Guo, Q., Su, Y., Hu, T., Zhao, X., Wu, F., Li, Y., Liu, J., Chen, L., Xu, G., Lin, G., Zheng, Y. i., Lin, Y., Mi, X., Fei, L., Wang, X., 2017. An integrated UAV-borne lidar system for 3D habitat mapping in three forest ecosystems across China. Int. J. Remote Sens. 38 (8-10), 2954–2972.

Guo, Q., Su, Y., Hu, T., Guan, H., Jin, S., Zhang, J., Zhao, X., Xu, K., Wei, D., Kelly, M., Coops, N.C., 2021. Lidar Boosts 3D Ecological Observations and modelings: a review and perspective. IEEE Geosci. Remote Sens. Mag. 9, 232–257. https://doi.org/10.1109/MGRS.2020.3032713.

Hu, T., Sun, X., Su, Y., Guan, H., Sun, Q., Kelly, M., Guo, Q., 2020. Development and performance evaluation of a very low-cost UAV-lidar system for forestry applications. Remote Sens. 13 (1), 77.

Jurado, J.M., Ramos, M.I., Feito, F.R., 2020. The impact of canopy feflectance on the 3d structure of individual trees in a mediterranean forest. Remote Sens. 12, 1430. https://doi.org/10.3390/rs12091430.

Luck, L., Hutley, L.B., Calders, K., Levick, S.R., 2020. Exploring the variability of tropical savanna tree structural allometry with terrestrial laser scanning. Remote Sens. 12 (23), 3893.

Mkaouar, A., Kallel, A., Rabah, Z.B., Chahed, T.S., 2021. Joint estimation of leaf area density and leaf angle distribution using TLS point cloud for forest stands. IEEE J. Sel. Top. Appl. Earth Obs. Remote Sens. 14, 11095–11115. https://doi.org/10.1109/JSTARS.2021.3120521.

Momo Takoudjou, S., Ploton, P., Sonké, B., Hackenberg, J., Griffon, S., Coligny, F., Kamdem, N.G., Libalah, M., Mofack, G.II., Le Moguédec, G., Pélissier, R., Barbier, N., McMahon, S., 2018. Using terrestrial laser scanning data to estimate large tropical trees biomass and calibrate allometric models: a comparison with traditional destructive approach. Methods Ecol. Evol. 9 (4), 905–916.

Muumbe, T.P., Baade, J., Singh, J., Schmullius, C., Thau, C., 2021. Terrestrial laser scanning for vegetation analyses with a special focus on savannas. Remote Sens. 13, 507. https://doi.org/10.3390/rs13030507.

Olagoke, A., Proisy, C., Féret, J.-B., Blanchard, E., Fromard, F., Mehlig, U., de Menezes, M.M., dos Santos, V.F., Berger, U., 2016. Extended biomass allometric equations for large mangrove trees from terrestrial LiDAR data. Trees 30, 935–947. https://doi.org/10.1007/s00468-015-1334-9.

Raumonen, P., Casella, E., Calders, K., Murphy, S., Åkerbloma, M., Kaasalainen, M., 2015. Massive-Scale Tree Modelling from Tls Data. ISPRS Annals of Photogrammetry, Remote Sensing and Spatial Information Sciences 3, 189–196. https://doi.org/10.5194/isprsannals-II-3-W4-189-2015.

Song, J., Zhu, X., Qi, J., Pang, Y., Yang, L., Yu, L., 2021. A method for quantifying understory leaf area index in a temperate forest through combining small footprint full-waveform and point cloud LiDAR data. Remote Sens. 13 (15), 3036.

Wang, J., Lindenbergh, R., Menenti, M., 2018. Scalable individual tree delineation in 3D point clouds. Photogram. Rec. 33, 315–340. https://doi.org/10.1111/phor.12247.